Microgravity Science and Technology (2019) 31:317–326
https://doi.org/10.1007/s12217-019-9685-2

ORIGINAL ARTICLE

Experimental Investigation on Effect of EDL on Heat Transfer of Micro Heat Pipe

Maryam Fallah Abbasi[1] · Hossein Shokouhmand[2]

Received: 25 May 2018 / Accepted: 5 February 2019 / Published online: 2 April 2019

Abstract

Due to the reduced dimensions of electronic equipment and the need for thermal management of these equipment, In order to increase efficiency and longevity of component, heat sinks with micro aspects are very important. In this study, heat transfer of micro heat pipe has been studied experimentally. For this purpose, firstly the micro heat pipe that is suitable for industrial conditions and restrictions for the production of very small size triangular section was designed and built. According to the very small size of the primary copper tube, the manufacturing process requires precision and advanced technology. In such a way, at first the samples of fine copper tube available in the market was provided and during the process of heat and tension was brought, at the same time, to the desired thickness and diameter and then by using provided wedge the appropriate cross section is achieved. To apply thermal load, a set of various thermal flux was applied to the evaporator and temperature distribution achieved via five thermocouples which were installed on the body in accordance with the set-up and heat resistance was measured. Water and different solution mixture of water and ethanol were used to investigate effect of the electric double layer heat transfer. It was noticed that the electric double layer of ionized fluid has caused reduction of heat transfer. So that the effect of the double electric layer causes 20% drop in the thermal performance of heat pipe. However, when the operating fluid was normal water or a mixture of water and ethanol, the temperature difference between the evaporator and the condenser was higher than when pure water used. This was due to the fact that the dual electrical layer led to a disruption in the flow path inside the pipe. Micro heat pipe performance was affected due to the small size of the micro pipe as well as the ions in the fluid, causing a higher temperature difference between the evaporator and condenser sections.

Keywords Heat transfer · Micro heat pipe · Electrical double layer · Magnetic field

Introduction

In recent decades, with the advent of micro scale manufacturing technology, many facilities for working with fluids in Nano liters scales have been created, and investing of the fluid flow has got high importance. Most famous of this equipment are micro heat pipes which are very small equipment that transfers thermal energy through phase changing. (Rahmat and Hubert 2010) The nominal diameters of these pipes, which are used to remove the heat of the small electronic packages, are 1.2 to 1.5 mm, and their length is about a few centimeters. Micro heat pipes are capable of not only transferring a large amount of heat but also creating uniform temperature which is because there is a two-phase fluid flow inside them.

As the volume of the liquid is decreasing in relative to its environment, some physical phenomenon like surface tension and surface charge are bolding which are negligible when they are in ordinary magnitude. Creating surface charge in the contact surface of solid and liquid causes an electrical double layer and non-uniform distributing of liquid ions near to surface. The electrical double layer forming and moving its charges with operating liquid, in transferring an electrolyte

This article belongs to the Topical Collection: Heat Pipe Systems for Thermal Management in Space
Guest Editors: Raffaele Savino, Sameer Khandekar

✉ Hossein Shokouhmand
hshokoh@ut.ac.ir

Maryam Fallah Abbasi
Mar.fallah@gmail.com

[1] Department of Mechanical Engineering, Science and Research Branch, Islamic Azad University, Tehran, Iran

[2] School of Mechanical Engineering, College of Eng. University of Tehran, Tehran, Iran

by means of the pressure-driving method inside a micro heat pipe, lead to Streaming phenomenon along the pipe (Mohiuddin Mala et al. 1997). M. Groll et al. have investigated several articles about the application of micro heat pipes for heat control of electrical equipment (Groll et al. 1998). M. Ivanova et al. studied micro silicon heat pipes characteristic with a triangular cross section (Ivanova et al. 2003). Saman et al. analyzed the performance of the micro heat pipes with a polygon cross-section. They showed that critical input heat decreases with increasing number of edges which lead to increase in friction coefficient, decreasing the velocity of flow and Capillary pumping capacity (Suman and Hoda 2005; Suman et al. 2005).

S. H. Moon et al. accomplished a complete survey about heat transferring in micro heat pipes. Their survey results about for micro copper pipe with triangular and square cross section illustrated that difference between the temperature of the evaporator and condenser increases as heat charge increases in special temperature. This is because vapor flow velocity increases with increasing of heat charge. Therefore, drag force in liquid-solid interface and pressure drop in fluid flow increases. Since the space for vapor flow in micro heat pipes is smaller than ordinary heat pipes, pressure drop resulted from friction in the liquid-vapor interface can extremely affect the performance of the micro heat pipes (Moon et al. 2004). Bhatti et al. investigated the entropy generation on electro-kinetically modulated peristaltic propulsion on the magnetized nano fluid flow through a micro channel with joule heating both theoretically and mathematically. (Bhatti et al. 2017a) Recently several authors investigated the effect of nanoparticles on heat transfer. (Sheikholeslami and Bhatti 2017a; b; Lei et al. 2017; Bhatti and Rashidi 2016; Vedavathi et al. 2017; Ren et al. 2001; Shahid et al. 2018; Heydari and Shokouhmand 2017; Shokouhmand et al. 2008).

Sheikholeslami et al. examined the nanofluid hydrothermal behavior in existence of external electric field and showed influence of electric field on forced convection improvement is more sensible for lower Re. (Sheikholeslami and Bhatti 2017a). Jhorar et al. presented a theoretical and mathematical study on pumping peristaltic through an asymmetric channel through an asymmetric channel. They showed that, with the increment in electro-osmotic parameter the potential function elevates whereas it opposes the velocity of the fluid. Phase difference reveals converse behavior on velocity profile whereas it significantly enhances the potential function (Jhorar et al. 2018). A few more studies on the EDL effect can be found from the references. (Gong et al. 2008; Bhatti et al. 2017b; Ganchenko et al. 2018; Sadiq and Joo 2009; Lee et al. 2010).

Governing Equations

Performance of the micro heat pipes resembles ordinary type. Evaporating of liquid absorbs heat from a thermal source in the evaporator. The vapor moves to condenser and condensates and releases heat. Micro heat pipes in contrast to ordinary ones instead of using sintered wick use sharp edges and grooves to bringing back liquid from evaporator to condenser. The solving area consists of liquid and vapor phases. Also, created electrical areas are effective in the whole solving area. There are two solving methods for liquid-vapor interface namely Lagrange and Euler. Lagrange method is limited to fluids with no incredible change of surface shape. Euler method has lower accuracy in relative to the Lagrange method, but it is capable of simulating fluids with a complicated interface and noticeable change in interface.

One of the most famous methods for solving a multiphase problem is VOF, which is also known as volume fraction method. This method allows the possibility of using the free surface of the interface between the two fluids and covering issues that exist in such matters, such as discontinuity or interfacial adhesion effects. In this method, a scalar function between zero and one is defined by the volume fraction function and is used to distinguish each of two phases. (Lei et al. 2017) (Figs. 1, 2, and 3).

Continuity Equation

$$\frac{\partial \rho}{\partial t} + \nabla \cdot (\rho v) = 0 \tag{1}$$

Momentum Equation

Momentum equation in the multi-phase environment is written in two forms. In the first form, it is derived separately for each phase based on the volume fraction of each phase and then equations are discretized and solved together (McGrath 2009; Mikelić 2009; Stevanović et al. 2007). In the second form which is known as fluid volume estimation (Youngs 1982), average density and viscosity according to volume

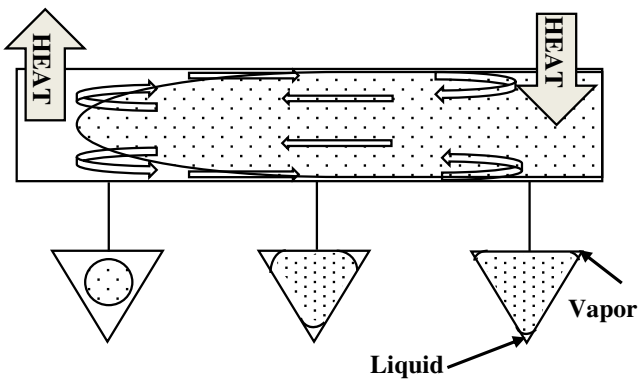

Fig. 1 The Schematic of the micro heat pipe function and utilizing groove to return the fluid from the evaporator to the condenser

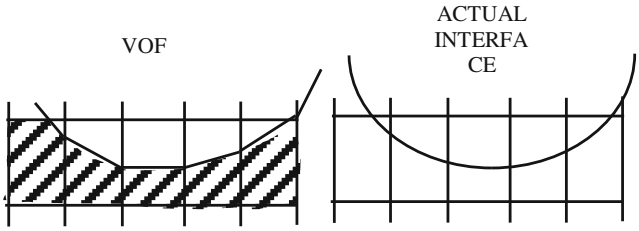

Fig. 2 The contact area of two phases in real mode (right) and by Eulerian VOF method (left)

fraction for vapor and liquid phase are used, and only one momentum equation including density and viscosity is derived (Yan and Che 2010; Delnoij et al. 1998).

$$\frac{\partial}{\partial t}(\rho v) + \nabla\cdot(\rho vv) = -\nabla \mathrm{p} + \nabla\cdot\left[\mu\left(\nabla v + \nabla v^{T}\right)\right] + \rho g + F + \sigma k \nabla \vec{n} \quad (2)$$

Where ρ and μ denote the density and the dynamic viscosity, respectively. The last term of Eq. (2) represents the surface tension force, with$k$,σ and $\vec{n}$ denoting the curvature (viewed from the gas phase), the Dirac delta function, and the unit normal vector of the interface (outward from the gas to liquid phases), respectively.

$$\frac{\partial}{\partial t}(\rho v) + \nabla\cdot(\rho vv) = -\nabla \mathrm{p} + \nabla\cdot(\mu\nabla v) + (\nabla v)\cdot\nabla\mu + \rho g + F + \sigma\kappa\nabla \vec{n} \quad (3)$$

Fluid Volume Method Equation

Equation of based on volume fraction,α is written as:

$$\frac{\partial \alpha}{\partial t} + \nabla\cdot(v\alpha) = 0 \quad (4)$$

Physical specification of the mixture is illustrated in Eq. (5) and (6):

$$\rho = \alpha\rho_l + (1-\alpha)\rho_g \quad (5)$$

$$\mu = \alpha\mu_l + (1-\alpha)\mu_g \quad (6)$$

Euler method of fluid volume method based on volume fraction transfer α and velocity of liquid and vapor phase velocity is written as follow (Cerne et al. 2001; Zhang and Qiu 2008)):

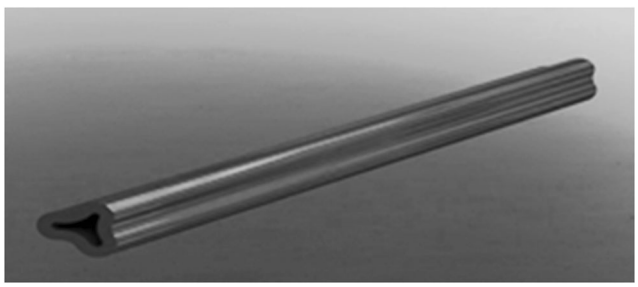

Fig. 3 Cross section of the micro heat pipe (triangular curves type)

Table 1 Specification of the micro heat pipe in experimental test

Cross section type	Triangular	Rectangular
Total length	50 (mm)	50 (mm)
Evaporator section length	10(mm)	10(mm)
Adiabatic section length	15(mm)	15(mm)
Condenser section length	25(mm)	25(mm)
Operating fluid	Water/water and ethanol mixture	Water/water and ethanol mixture
Number of corners	3	4
Micropipe material	Free-oxygen cupper	Free-oxygen cupper

$$\frac{\partial \alpha}{\partial t} + \nabla\cdot(v_l\alpha) = 0 \quad (7)$$

$$\frac{\partial(1-\alpha)}{\partial t} + \nabla\cdot\left[v_g(1-\alpha)\right] = 0 \quad (8)$$

Where l and g illustrate the velocity of the liquid and vapor phase respectively,

$$v = \alpha v_l + (1-\alpha)v_g \quad (9)$$

The integrated equation for fluid volume method in the two-phase area of liquid and vapor is obtained as:

$$\frac{\partial \alpha}{\partial t} + \nabla\cdot(v\alpha) + \nabla\cdot[v_r\alpha(1-\alpha)] = 0 \quad (10)$$

Energy Equation

$$\frac{\partial}{\partial t}\left(\rho c_p T\right) + \nabla\cdot\left(v\left(\rho c_p T + \mathrm{p}\right)\right) = \nabla\cdot\left(k_{eff}\nabla T\right) + S_h \quad (11)$$

In the above equation, S_h is any heating source including radiation and k_{eff} is Effective Thermal Conductivity. T illustrates temperature which is calculated for liquid and vapor phase like:

$$T = \alpha T_1 + (1-\alpha)T_g \quad (12)$$

Conductive Heat Transfer(Wall)

The wall has Conductive heat transfer whose equation is obtained as:

$$q''' + \nabla(k_s\nabla T) = \left(\rho C_p\right)_s \frac{\partial T}{\partial t} \quad (13)$$

Where q''' is heat generated by the thermal source is, k_s is the thermal conductivity coefficient of the wall and Cp is specific heat.

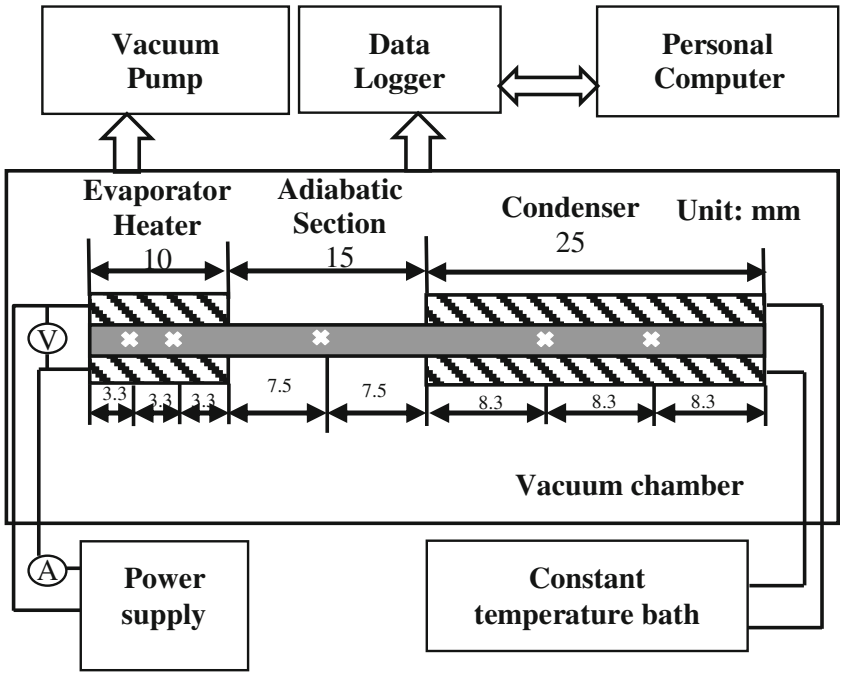

Fig. 4 Set-up used in research

Effect of Body Forces

If ϕ is external electrical potential on micro heat pipe, body force generated by it is obtained as (Zhang and Qiu 2008):

$$f_1 = \rho_e E = \rho_e \nabla\phi \tag{14}$$

$$\rho_e = \varepsilon\varepsilon_0 \mathbf{k}^2 \psi_1 \tag{15}$$

$$\mathbf{k} = \sqrt{\frac{\mathbf{F}^2}{\varepsilon RT}\sum_i z_i^2 c_{i,0}} \tag{16}$$

In the above equation, **k** is the inverse of Debye length, **F** is the Faraday constant, R is the universal gas constant, T is the absolute temperature and $c_{i,\,0}$ is the bulk concentration of the ith ion. Respectively $\psi_1$the potential of the wall recharge. Ψ2 is the electric potential and ρ_e volumetric charging of the double electrical layer, resulting from liquid and solid contact with the symmetry condition, are expressed by (Ren et al. 2001; Gong et al. 2008; Bhatti et al. 2017b).

ε is the dielectric coefficient, n_0 is the bulk ionic concentration, z is and the valence of ions, e is the charge of a proton, k_b is Boltzmann's constant, and T is absolute temperature. Body force generated by an electrical double layer between the liquid and solid phase is calculated as:

$$\nabla^2\psi_2 = -\frac{2n_0 ze}{\varepsilon} sinh\left(-\frac{ze\psi_2}{k_b T}\right) \tag{17}$$

$$\rho_e = -\varepsilon\nabla^2\psi_2 = -2n_0 zesinh\left(-\frac{ze\psi_2}{k_b T}\right) \tag{18}$$

$$f_2 = \rho_e E \tag{19}$$

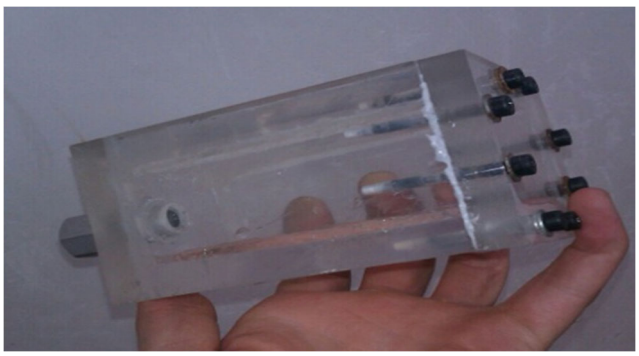

Fig. 5 Vacuum chamber which used in the test

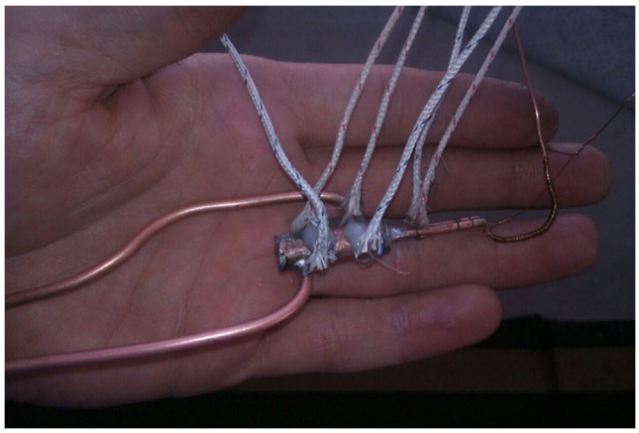

Fig. 6 The location and installation of thermocouple

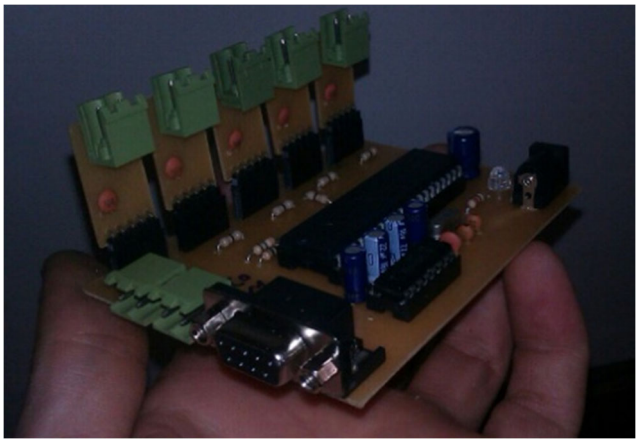

Fig. 7 Micro heat pipe adapter

E is the electro viscous force. Double electrical layer force between liquid and vapor phase can be written as (Nakajima 2011):

$$f_3 = \underbrace{-\frac{a}{2}\psi_3^2 + \frac{b}{4}\psi_3^4 - cz_i eV_e\psi_3}_{\text{homogeneous system}} + \underbrace{\frac{d}{2}(\nabla\psi_3)^2}_{\text{inhomogeneous system}} \tag{20}$$

$$a = \frac{U_{sum} - 4k_sT}{l^3}, b = \frac{16k_sT}{3l^3}, c = \frac{1}{2l^3}, d = \frac{U_{sum}}{2l^3}$$

$$\mu^S = \mu^{-S} + q\psi_3 \tag{21}$$

In the above relation, μ^S is the chemical potential of ions at the contact level and q is the charge of the ion. In this study we have different electronic forces which have a strong effect on the field of gravity .all of these forces are:

$$F = f_1 + f_2 + f_3 \tag{22}$$

The Setup Used in Research

Micro heat pipe manufacturing was complicated because of having small dimensions. In this investigation, two types of copper micro pipes with triangular and rectangular cross-section were used. Cross section and diameter of pipes were reached to specified values before reforming by heating and applying tension (Table 1).

After designing and producing micro pipe, we had to fill in the pipes with operating fluid. Non-condensable gases in heat pipe could disrupt fluid flow and heat pipe performance. In the worst situation, fluid circulation ceased, and heat pipes missed their performance and acted as a conductive. To avoid this problem when manufacturing of required samples, at first the end of sample micro heat pipes, more than the length required had to block and evacuating might be done from another end. Subsequently, 20% of the micro heat pipes volume was filled with fluid; after cutting redundant part and blocking the beginning, leakage test was done. Micro heat pipe experiment device consisted of vacuum chamber, a heat transforming system for the cooling condenser, the evaporator with a heater, made up of a wire with 0.36 diameter and 10 M/X resistance per meter for providing constant heat charge, data acquisition system and thermocouples for measuring temperature (Fig. 4). The vacuum chamber was made of acrylic to reduce heat waste as shown in Fig. 5.

Type K thermocouple (0.08 mm) was placed by soldering in two sections in the evaporator wall, one point in the adiabatic section, and two points in the condenser (Fig. 6). The locations of this thermocouple are shown as X in Fig. 4. The micro heat pipe was made of oxygen-free copper and had a wall thickness between 0.27 and 0.28 mm.

Pure water, ordinary water and in the next step a various mixture of water and Ethanol were used as an operating fluid, with a relatively large surface tension and a special latent heat between 30 to 160 degrees Celsius.

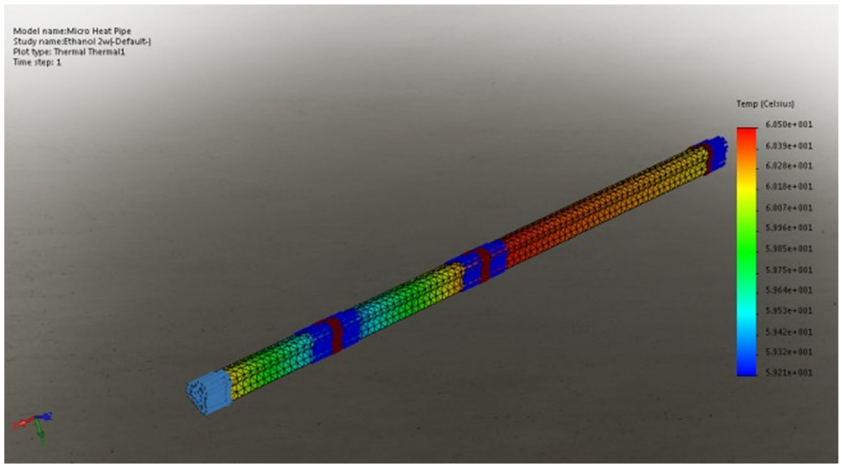

Fig. 8 Meshing that used for boundary conditions

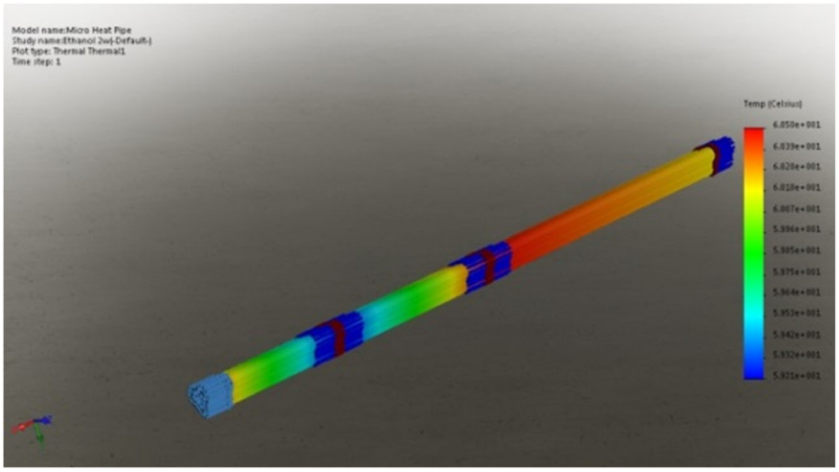

Fig. 9 Thermal contour for input current

20% of Micro heat pipe volume was filled with fluid. The blocking region of the liquid in which the vapor was not possible could be created in the condenser. Heat transferring could not be completed by changing the fluid phase in the closed area of the fluid. The temperature in the condenser end was 5 to 20 degrees Celsius less than the area adjacent to the condenser and the heat transfer rate of the micro-heat pipe was reduced due to fluid blockage. Therefore, the inactive amount of operating fluid due to blockage of fluid should be considered in the design stage of the micro heat pipe to calculate the fluid filling ratio. An adapter as one shown in Fig. 7 was used to calibrate the sensors aiming to display their values.

Heat Transfer Characteristics of the Micro Heat Pipe

The heat pipe could transmit a large amount of heat with a small temperature difference between the evaporator and the condenser. Measuring the temperature difference between the evaporator and the condenser was an indicator to check whether there was a non-condensable gas in the heat pipe or heat pipe worked well. However, we might remember that each heat pipe has a special temperature difference. High precision technologies were needed in the production process of small heat pipes like present study, because the presence of non-condensable or polluting gases, even at a low amount, could be detrimental to the performance of the heat pipes.

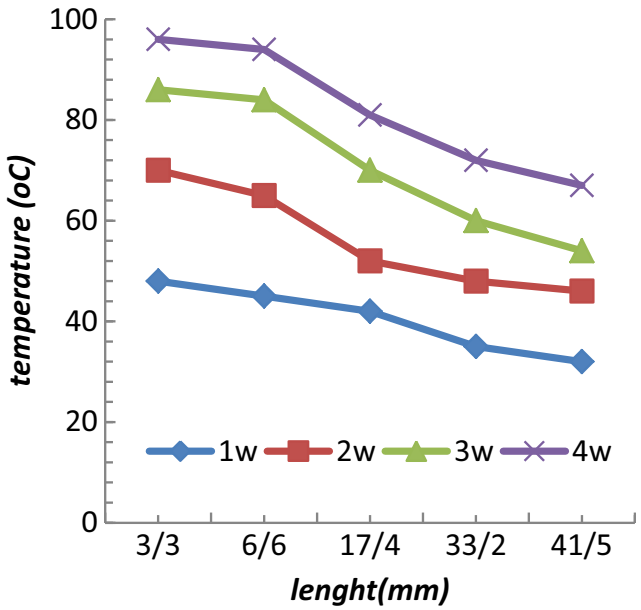

Fig. 10 Temperature distribution in the axial length of 50 mm in the micro pipe - working fluid of ordinary water

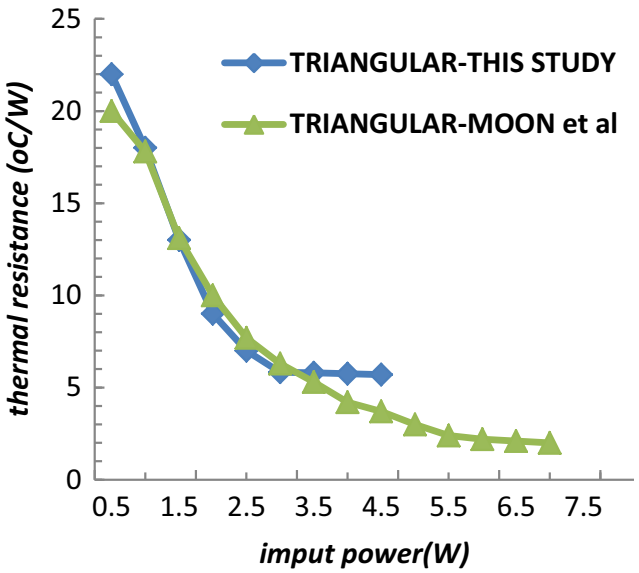

Fig. 11 Validation of sample thermal resistance tested with previous record and researches

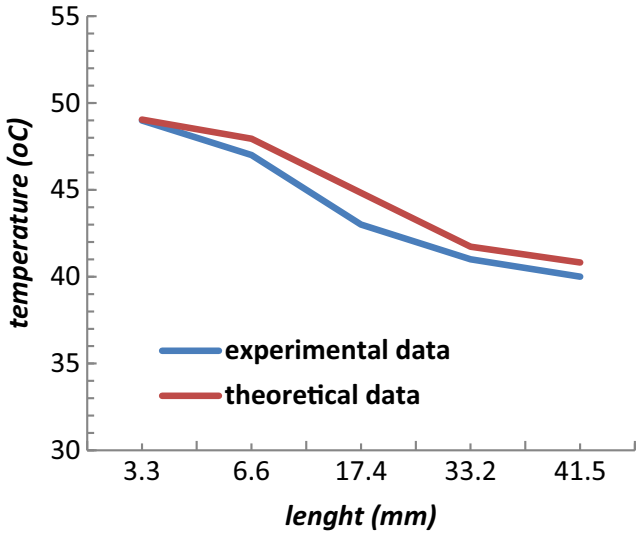

Fig. 12 Compare experimental and theoretical graph of wall temperature, water and ethanol 0.018 as working fluid, 1 W

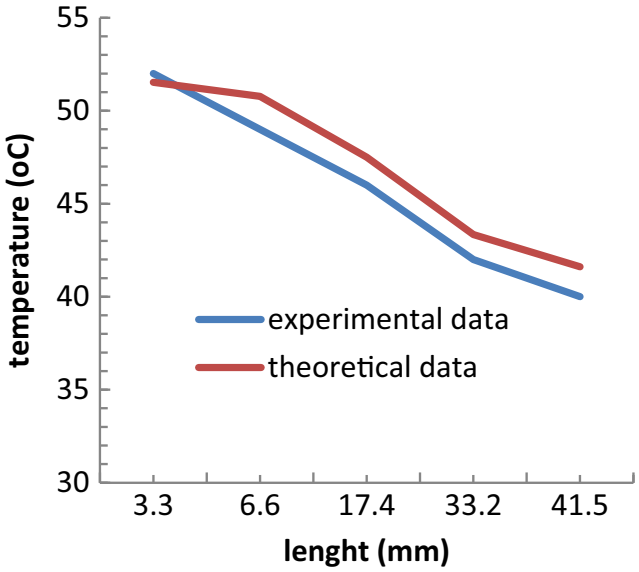

Fig. 14 Compare the experimental and theoretical graph of wall temperature, water and ethanol 0.054 as working fluid, 1 W

Simulated Model with Software

Due to the operation conditions of the research sample and also equations developed in the second section, the results of software simulation are presented in the following. It was worth noting that Electrical double layer effects were not considered by the software. AutoCAD software was used to draw the geometry of micro pipe and then mentioned geometry was imported to fluent software as a DXF standard output format. Excel software was used to draw curves. Figure 8 shows the mesh used for analysis.

Figure 9 shows Temperature distribution in the axial length of 50 mm in micro heat pipe with a triangular cross-section. The test micro heat pipe had a curved triangle cross-section with a filling ratio of 20% to the total internal volume. The heat was only dissipated in the condenser by conduction. The temperature after the steady state area was averaged to reduce fluctuation error.

As shown in Fig. 10, the temperature of the micro heat pipe walls increased with increase in heat charge which indicated that uniform temperature from the evaporator to the condenser was truly established. The temperature difference between the evaporator and the condenser in different heat charge was shown in the following figures.

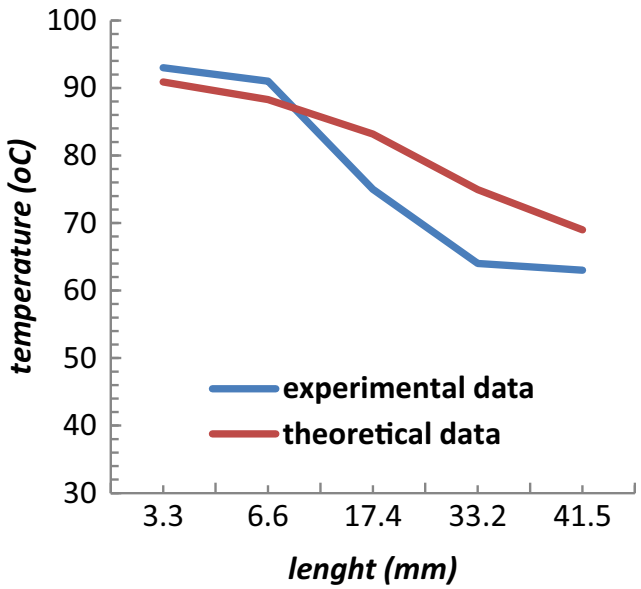

Fig. 13 Compare the experimental and theoretical graph of wall temperature, water and ethanol 0.018 as working fluid, 4 W

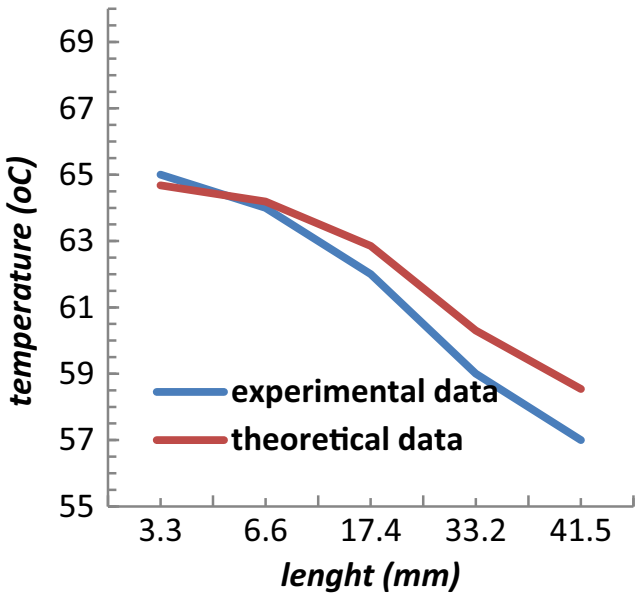

Fig. 15 Compare the experimental and theoretical graph of wall temperature, water and ethanol 0.054 as working fluid, 2 W

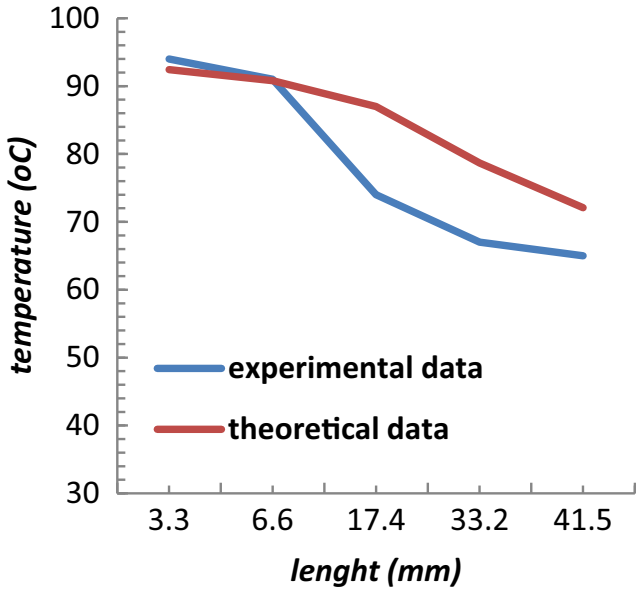

Fig. 16 Compare the experimental and theoretical graph of wall temperature, water and ethanol 0.054 as working fluid, 4

However, when the operating fluid was normal water or a mixture of water and ethanol, the temperature difference between the evaporator and the condenser was higher than when pure water used. This was due to the fact that the dual electrical layer led to a disruption in the flow path inside the pipe. Micro heat pipe performance was affected due to the small size of the micropipe as well as the ions in the fluid, causing a higher temperature difference between the evaporator and condenser sections.

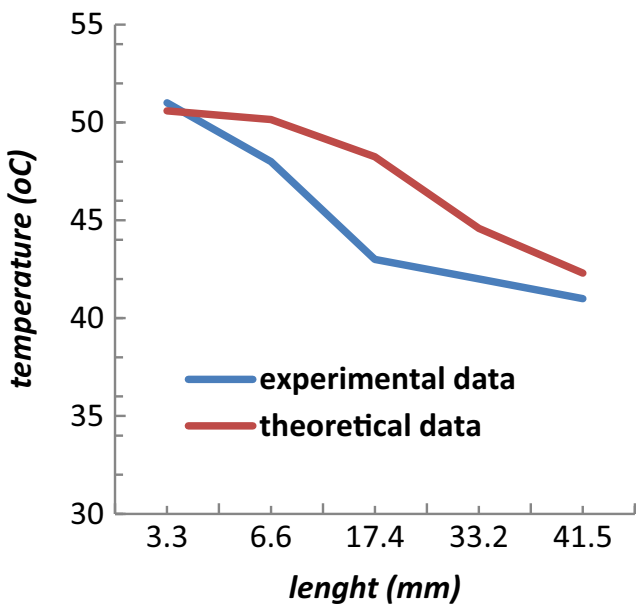

Fig. 17 Compare the experimental and theoretical graph of wall temperature, water /water and ethanol 0.18 as working fluid, 1 W

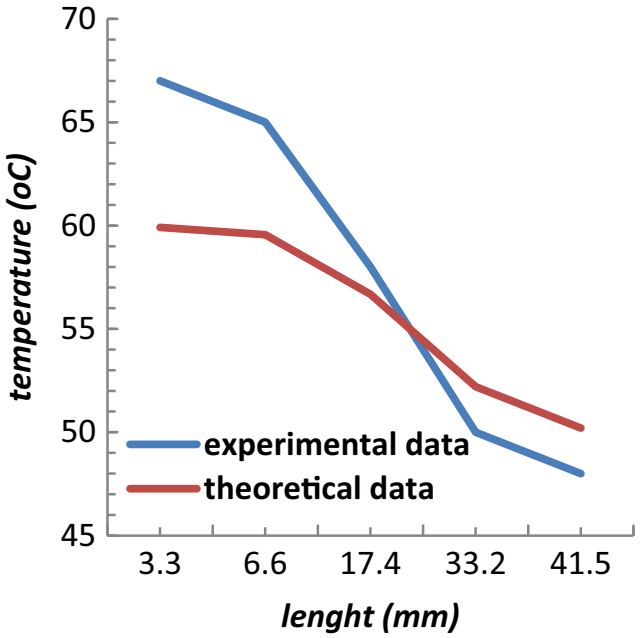

Fig. 18 Compare the experimental and theoretical graph of wall temperature, water /water and ethanol 0.18 as working fluid, 2 W

Discussion and Conclusion

Micro heat pipes with polygon cross-section usable in electronic devices were produced and tested. High profitability and easy production procedure are considered for future application. Micro heat pipes with pure water showed uniform temperature characteristic through the pipe, and the

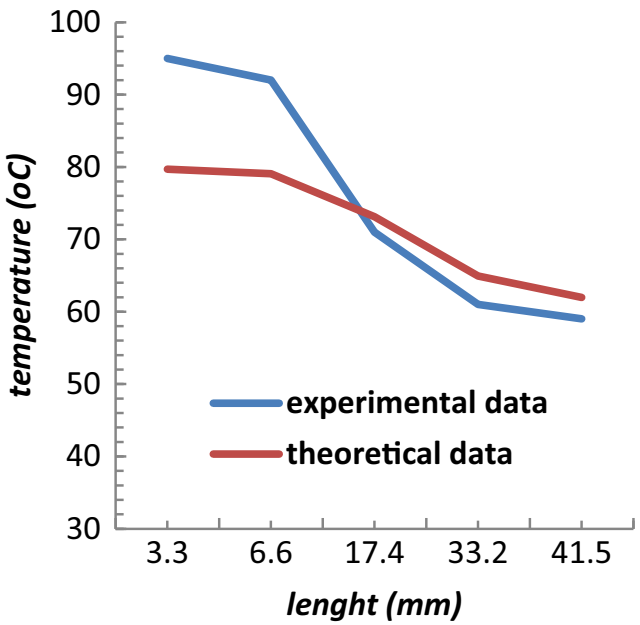

Fig. 19 Compare the experimental and theoretical graph of wall temperature water /water and ethanol 0.18 as working fluid, 4 W

temperature difference between the evaporator and the condenser was between 11 to 16 degrees Celsius.

The effect of the slope angle on the thermal performance was low and the thermal characteristics were stable. The effect of length was noticeable on the thermal performance of the micro heat pipe. Wall temperature was higher when normal water was used. This indicated the effect of the dual electric layer in the case of using ordinary water. In the present study, the heat dissipation capacity was high, and also it was showed that in the pipes with small dimensions, the effect of the double electric layer causes 20% drop in the thermal performance of heat pipe.

It could be widely used in integrated electronic devices as a cooling unit. In order to verify the used layout and compare the results with the references and previous studies, the heat pipes set was tested with the same fluids as a reference (Moon et al. 2004) and the accuracy of the heat pipes set performance was confirmed (Fig. 11).

In order to measure the effect of a dual electric layer on the heat transfer inside the micro pipe, due to the effect of alcohol concentration in water and alcohol solution, in the experimental tests and numerical studies, different solutions of water and alcohol were used. Due to the very small dimensions of the micro heat pipe, producing of the heat pipe and injecting the fluid into it had special complexities which have been coped with carefully by allocating a large amount of time.

By comparing experimental and simulation results where input power was 1 watt and using a water-ethanol mixture with 1 drop of ethanol equal to 0.018 g, were observed that the average difference between the results was less than 0.7 degree and the highest difference was 4% in the adiabatic region (Fig. 12). By increasing the input power from 1 to 4 watts, it was observed that the difference between the experimental and simulation results increased so that the least difference was more than 2% and at most it reached 17% (Fig. 13). In this case, for an input power of 1 and 2 watts, dual electric layer effect caused no significant difference. But in the power of 4 watts, in addition to the difference between the experimental and simulation results due to the presence of the dual electric layer, the temperature difference between the evaporator and the condenser also increased by 27% (Fig. 13).

Regarding this fact that dual electric layer effect was expected to increase with an increase in alcohol concentration; ethanol concentration was increased to 3 times by using 0.054 g of alcohol. In power input of 1 watt, the difference in experimental and simulation results increased so that the average difference was 5% (Fig. 14). This difference was observed in all diagrams and power ranges.

According to Fig. 13, in comparison with the ethanol concentration of 0.018, the temperature difference between the two ends of the micro heat pipe increased in experimental and simulation tests (Figs. 15 and 16). This difference was more noticeable at the power of 4 watts and it reached 30% which could be due to this fact that the larger flow the larger phase change. In the highest concentration with 0.18% of alcohol, as shown in the diagrams, theoretically, there was a lower temperature difference between the evaporator and the condenser in all input power ranges. As the input power increased, this difference also increased (Figs. 17, 18 and 19).

Nomenclature v, Velocity (m/s); v_l, Velocity of the liquid (m/s); v_g, Velocity of the vapor (m/s); v_r, The difference between the velocity of the liquid phase and the vapor phase velocity $V_L - v_G$ (m/s); t, Time (s); P, Pressure(Pa); $\boldsymbol{T}$, Matrix transpose; g, Acceleration of gravity (m/s^2); F, Body force (N); f_1, The force caused by an external electric potential (N); f_2, Body force generated by an electrical double layer between the liquid and solid (N); f_3, Body force generated by an electrical double layer between the liquid and vapor (N); E, Electro viscous force (N); k, The curvature (viewed from the vapor phase); $\mathbf{k}$, The inverse of Debye length (m^{-1}); k_b, Boltzmann's constant (1.3×10^{-3}); $\vec{n}$, The unit normal vector of the interface (outward from the gas to liquid phases); S_h, Any heating source including radiation and (W/m^3); k_{eff}, Effective thermal conductivity (W/(m.K)); T, Temperature (K); q''', Heat generated by the thermal source (W/m$^{3)}$; k_s, Thermal conductivity coefficient of the wall (W/(m.K)); C_p, Specific heat (J/(kg.K)); k, Inverse of Debye length (1/m); $\boldsymbol{F}$, Faraday constant ($9.65 \times 10^{4)}$; R, Universal gas constant (8.314×103 J/(mol.K)); $c_{i,\,0}$, Bulk concentration of the ith ion; n_0, Bulk ionic concentration,; z, Valence of ions; e, Charge of a proton; q, Charge of the ion; l, Liquid; g, Gas

Greek Symbol ρ, Density (Kg/m$^{3)}$; ρ_e, Volumetric charging of the double electrical layer (C/m^2); μ, Dynamic viscosity (Pa.s); σ, Coefficient of contact surface tension (N/m); α, Volume fraction; ϕ, External electrical potential (V); ψ_1, Potential of the wall recharge (V); ψ_2, Electric potential (V); ε, Dielectric coefficient (C/m^3); μ^S, Chemical potential of ions at the contact level (J/mol)

References

Bhatti, M.M., Rashidi, M.M.: Effects of thermo-diffusion and thermal radiation on Williamson nanofluid over a porous shrinking/stretching sheet. J. Mol. Liq. **221**, 567–573 (2016). https://doi.org/10.1016/j.molliq.2016.05.049

Bhatti, M., Sheikholeslami, M., Zeeshan, A.: Entropy analysis on electrokinetically modulated peristaltic propulsion of magnetized nanofluid flow through a microchannel. Entropy. **19**(9), 481 (2017a)

Bhatti, M.M., Zeeshan, A., Ellahi, R., Ijaz, N.: Heat and mass transfer of two-phase flow with electric double layer effects induced due to peristaltic propulsion in the presence of transverse magnetic field. J. Mol. Liq. **230**, 237–246 (2017b). https://doi.org/10.1016/j.molliq.2017.01.033

Cerne, G., Petelin, S., Tiselj, I.: Coupling of the interface tracking and the two-fluid models for the simulation of incompressible two-phase flow. J. Comput. Phys. **171**(2), 776–804 (2001). https://doi.org/10.1006/jcph.2001.6810

Delnoij, E., Kuipers, J.A.M., Vassilicos, J.C.: Numerical simulation of bubble coalescence using a volume of fluid (VOF) model. In: CONF (1998)

Ganchenko, G., Frants, E., Shelistov, V., Demekhin, E.J.M.S.: Technology: the movement of an ion-exchange microparticle in a weak external electric field. **30**(4), 411–417 (2018). https://doi.org/10.1007/s12217-018-9627-4

Gong, L., Wu, J.-k., Wang, L., Chao, K.: Periodical streaming potential and electro-viscous effects in microchannel flow. Appl. Math. Mech. **29**(6), 715–724 (2008). https://doi.org/10.1007/s10483-008-0603-7

Groll, M., Schneider, M., Sartre, V., Chaker Zaghdoudi, M., Lallemand, M.: Thermal control of electronic equipment by heat pipes. Revue Générale de Thermique. **37**(5), 323–352 (1998). https://doi.org/10.1016/S0035-3159(98)80089-5

Heydari, M., Shokouhmand, H.: Numerical study on the effects of variable properties and nanoparticle diameter on nanofluid flow and heat transfer through micro-annulus. Int. J. Numer. Methods Heat Fluid Flow. **27**(8), 1851–1869 (2017)

Ivanova, M., Schaeffer, C., Avenas, Y., Lai, A., Gillot, C.: Realization and thermal analysis of silicon thermal spreaders used in power electronics cooling. In: IEEE International Conference on Industrial Technology, 2003, 10–12 Dec. 2003, vol. 1122, pp. 1124–1129 (2003)

Jhorar, R., Tripathi, D., Bhatti, M.M., Ellahi, R.: Electroosmosis modulated biomechanical transport through asymmetric microfluidics channel. **92**(10), 1229–1238 (2018). https://doi.org/10.1007/s12648-018-1215-3

Lee, S.Y., Yalcin, S.E., Joo, S.W., Sharma, A., Baysal, O., Qian, S.J.M.S.: Technology: the effect of axial concentration gradient on electrophoretic motion of a charged spherical particle in a nanopore. **22**(3), 329–338 (2010). https://doi.org/10.1007/s12217-010-9195-8

Lei, Y., Chen, Z., Shi, J.J.M.S.: Technology: analysis of condensation heat transfer performance in curved triangle microchannels based on the volume of fluid method. **29**(6), 433–443 (2017). https://doi.org/10.1007/s12217-017-9562-9

McGrath, T.P.: Effect of volume fraction evolution on the mathematical model for compressible multiphase FLOWS. AIP Conference Proceedings. **1195**(1), 95–98 (2009). https://doi.org/10.1063/1.3295304

Mikelić, A.: An existence result for the equations describing a gas–liquid two-phase flow. Comptes Rendus Mécanique. **337**(4), 226–232 (2009). https://doi.org/10.1016/j.crme.2009.04.007

Mohiuddin Mala, G., Li, D., Dale, J.D.: Heat transfer and fluid flow in microchannels. Int. J. Heat Mass Transf. **40**(13), 3079–3088 (1997). https://doi.org/10.1016/S0017-9310(96)00356-0

Moon, S.H., Hwang, G., Ko, S.C., Kim, Y.T.: Experimental study on the thermal performance of micro-heat pipe with cross-section of polygon. Microelectron. Reliab. **44**(2), 315–321 (2004). https://doi.org/10.1016/S0026-2714(03)00160-4

Nakajima, H. (ed.): Mass transfer - advanced aspects. InTech, Rijeka (2011)

Rahmat, M., Hubert, P.: Two-phase simulations of micro heat pipes. Comput. Fluids. **39**(3), 451–460 (2010). https://doi.org/10.1016/j.compfluid.2009.09.014

Ren, L., Li, D., Qu, W.: Electro-viscous effects on liquid flow in microchannels. J. Colloid Interface Sci. **233**(1), 12–22 (2001). https://doi.org/10.1006/jcis.2000.7262

Sadiq, I.M.R., Joo, S.W.: Weakly nonlinear stability analysis of an electro-osmotic thin film free surface flow. Microgravity Sci. Technol. **21**(1), 331–343 (2009). https://doi.org/10.1007/s12217-009-9110-3

Shahid, A., Zhou, Z., Bhatti, M.M., Tripathi, D.: Magnetohydrodynamics nanofluid flow containing gyrotactic microorganisms propagating over a stretching surface by successive taylor series linearization method. Microgravity Sci. Technol. **30**(4), 445–455 (2018). https://doi.org/10.1007/s12217-018-9600-2

Sheikholeslami, M., Bhatti, M.M.: Active method for nanofluid heat transfer enhancement by means of EHD. Int. J. Heat Mass Transf. **109**, 115–122 (2017a). https://doi.org/10.1016/j.ijheatmasstransfer.2017.01.115

Sheikholeslami, M., Bhatti, M.M.: Forced convection of nanofluid in presence of constant magnetic field considering shape effects of nanoparticles. Int. J. Heat Mass Transf. **111**, 1039–1049 (2017b). https://doi.org/10.1016/j.ijheatmasstransfer.2017.04.070

Shokouhmand, H., Ghazvini, M., Shabanian, J.: Performance Analysis of Using Nanofluids in Microchannel Heat Sink in different Flow Regimes and its simulation using Artificial Neural Network. Proceedings of the World Congress on Engineering 2008 Vol III, WCE 2008, July 2–4, 2008, London, U.K.

Stevanović, V., Prica, S., Maslovarić, B.: Multi-fluid model predictions of GasLiquid two-phase flows in vertical tubes. FME Transactions. **35**(4), 173–181 (2007)

Suman, B., Hoda, N.: Effect of variations in thermophysical properties and design parameters on the performance of a V-shaped micro grooved heat pipe. Int. J. Heat Mass Transf. **48**(10), 2090–2101 (2005). https://doi.org/10.1016/j.ijheatmasstransfer.2005.01.007

Suman, B., De, S., DasGupta, S.: A model of the capillary limit of a micro heat pipe and prediction of the dry-out length. Int. J. Heat Fluid Flow. **26**(3), 495–505 (2005). https://doi.org/10.1016/j.ijheatfluidflow.2004.09.006

Vedavathi, N., Balamurugan, K.S., Gurram, D.: Heat transfer on mhd nanofluid flow over a semi infinite flat plate embedded. Frontiers in Heat and Mass Transfer. (2017)

Yan, K., Che, D.: A coupled model for simulation of the gas–liquid two-phase flow with complex flow patterns. Int. J. Multiphase Flow. **36**(4), 333–348 (2010). https://doi.org/10.1016/j.ijmultiphaseflow.2009.11.007

Youngs, D.L.: Time-dependent multi-material flow with large fluid distortion. Numerical Methods for Fluid Dynamics. (1982)

Zhang, P., Qiu, H.H.: Investigation of the patterned surface modification on 3D vortex flow generation in a micropipe. J. Micromech. Microeng. **18**(11), 115030 (2008)